# Magnetic properties of finite superconducting cylinders. I. Uniform applied field

Alvaro Sanchez[1] and Carles Navau[1,2]
[1]*Grup d'Electromagnetisme, Departament de Física, Universitat Autònoma Barcelona, 08193 Bellaterra (Barcelona), Catalonia, Spain*
[2]*Escola Universitària Salesiana de Sarrià, Rafael Batlle 7, 08017 Barcelona, Catalonia, Spain*
(Received 13 March 2001; published 1 November 2001)

A model for the calculation of the magnetic levitation force for finite type-II superconductors in the critical state is presented in a series of two papers. In the first paper, we describe the main features of the model and understand the effect of demagnetizing fields in the magnetic properties of finite superconductors by considering the case of a superconducting cylinder in the presence of a homogeneous applied field. Field and current profiles are calculated from a minimization of the magnetic energy in the superconductor after a change in the applied field. Results are presented for both constant and field-dependent critical currents. The procedure is general enough to be applied to the case of nonuniform applied fields, as long as the cylindrical geometry is preserved.

DOI: 10.1103/PhysRevB.64.214506 PACS number(s): 74.60.Jg, 85.25.Ly

## I. INTRODUCTION

Stable magnetic levitation is one of the most impressive exhibitions of the unique properties of superconductors.[1] Magnetic levitation forces result from the interaction between an external magnetic field and the currents in the superconductor. Although type-I superconductors can levitate, the most interesting case for the study and application of the levitation phenomena is that of type-II superconductors, for which the levitation is ''rigid'' for a wide range of positions and orientations of the superconductor.[1–3] However, even in the simple case of a superconductor (SC) levitating over a permanent magnet, the modeling and understanding of the levitation force is complicated by factors such as the nonlinear response of the type-II superconductor to the field of the magnet and the demagnetizing effects arising from the magnetic poles at the surfaces of the superconductor.

A successful model of superconducting levitation thus requires an adequate treatment of the magnetization of the superconductor which results from the application of a magnetic field. In general, owing to the complexity of the microscopic description of the vortex state, the magnetic response of type-II SC's has been studied by means of approximations which describe the observed macroscopic behavior. The most common approach is the critical-state model,[4] which assumes that the currents circulating in the SC's flow with a density that only depends upon the local magnetic field, $J=J_c(H_i)$. It has been found that the critical-state model adequately describes the magnetic properties of granular and melt-textured samples of high-$T_c$ superconductors with a strong $J_c(H_i)$ dependence which is often well described by an exponential decay.[5,6] These types of samples are the most used in levitation experiments.

Important advances were recently made in the modeling of macroscopic magnetic properties of finite superconductors, for which the study of the demagnetizing effects has to be included. Brandt[7] and Doyle *et al.*[8] presented methods of solutions for the magnetization of finite cylinders and disks, based on assuming that the superconductor response arises from macroscopic material laws $B(H)$ and $J(E)$. However, these methods were not applied to the case of spatially inhomogeneous applied fields, as required for levitation experiments. Actually, the models for superconducting levitation presented up to now have not solved the demagnetization problem. All these models either neglected the effect of demagnetizing fields (such as in Refs. 9–12) or considered them by the simple approximation of a constant demagnetization factor,[13] with the exception of works dealing with thin-film geometry, for which demagnetizing effects were considered.[14,15] In the second paper of this series we will provide a brief survey of the theoretical models proposed for describing the superconductor levitation; from this, one can conclude that a complete model of superconducting levitation has not been proposed till now.

Our aim in this series of papers is to introduce a realistic model for the levitation of superconductors in the presence of an external spatially inhomogeneous magnetic field. The model is based on calculating current profiles in the superconductor by a minimization of its magnetic energy after a change in the applied field. In this first paper of this series we describe the model, and present a systematic study of the magnetization of a type-II superconductor resulting from a spatially uniform applied magnetic field as a function of some of the superconductor parameters, in order to discuss the main features of the magnetic response of the superconductors associated with the demagnetizing effects. In the second paper we use the basic formalism presented here to study the case of inhomogeneous fields, from which levitation forces occur for the superconductor. Although the model is readily applicable to any system with cylindrical symmetry, the calculations and results in this work will deal with the most typical case encountered in levitation experiments, which is the case of a superconductor levitating in the field of a coaxial permanent magnet.

The validity of the model results will be checked in two different forms. First, for the case of a constant applied magnetic field, we will compare the model results with both the analytical formulas that are known for the limits of infinitely long cylinders[16] and very thin disks,[17] and, for superconductors of intermediate size, with those obtained from other numerical approaches.[7] A very satisfactory agreement is obtained in all cases (see Sec. VI A of this paper). Second,

 

results corresponding to nonuniform applied fields and levitation forces are compared with both analytical expressions in some limits and experimental levitation force curves and other features observed in actual experiments. As we discuss in Sec. V of the second paper, we find that our model describes the characteristics experimentally found.

This paper is structured as follows. In Sec. II we discuss the general properties of superconductors in the critical state. In Sec. III, we describe the model details. The model results are presented for two different cases: in Sec. IV we discuss the case of constant $J_c$ in order to analyze the influence of demagnetizing effects in the simplest situation, whereas we devote Sec. V to a study of the more general case of $J_c$ depending upon the local field $J_c(H_i)$. In Sec. VI we compare some of our results with both experimental results and theoretical predictions from other existing theories, in several limits. The conclusions of the first part of this work are presented in Sec. VII.

## II. MACROSCOPIC VIEW OF SUPERCONDUCTORS IN THE CRITICAL STATE

From a macroscopic point of view, superconductors present two main characteristic magnetic behaviors. When they are cooled through the critical temperature in the presence of an applied magnetic field, the magnetic flux present in the superconductor interior is expelled (Meissner effect). The other important effect, the one in which we are interested here, occurs when a magnetic field is applied to a SC under isothermal conditions; the SC reacts by excluding the magnetic field in its interior, so that the total magnetic field $B$ is equal to zero in the bulk of the SC. For type-II superconductors with pinning, a complete magnetic shielding (except for a surface region of depth $\lambda$ at the surfaces, where shielding current flows) occurs when the total field is below the value of the lower critical field $B_{c1}$. For higher fields, there appear some bulk currents which tend to shield the interior region, that is, to make the internal field $\mathbf{H}_i=\mathbf{B}/\mu_0=0$ there. Wherever there are currents, $\mathbf{B}\neq 0$. So, two regions appear: (a) an interior region with neither magnetic field nor bulk currents, and (b) an exterior region with a magnetic field and current different from zero (in the critical-state model, the value of the current in this region is the critical one). Further increasing the applied field makes the central field-free region shrink, until it eventually vanishes. If the sense of the sweeping rate of the external applied field is reversed (reverse curve) the effect on the superconductor is the same: induced supercurrents tend to shield the interior of the superconductor, that is, to preserve the field distribution already present. So the two regions are now (a) a frozen-field interior region, and (b) an exterior region with a critical current and a modified internal field.

We can summarize the previous behavior by considering that type-II superconductors in the critical state behave macroscopically after a quasistatically variation of an external applied field as follows: a macroscopic current is set in the SC in order to shield the magnetic field in the largest possible region inside the superconductor. Since the current has a maximum possible density $J_c(H_i)$, when the applied field is modified, the superconductor responds by pushing the current front inward.

In the virgin magnetization curve, shielding the magnetic field in the superconductor volume by induction of currents is equivalent to minimizing the magnetic energy resulting from the application of the applied field. Then, in order to simulate the macroscopic process, in our model we find a current-penetrated region that ensures the maximum shielding for each value of the applied field by finding the regions at which setting a current with value $J_c(H_i)$ minimizes the magnetic energy. The minimization of the energy for finding the macroscopic magnetic properties of type-II superconductors was used by Badia *et al.*[18] For the reverse curve, we shall simulate the magnetic shielding by the conventional critical-state model procedure of superimposing a current distribution with opposite sign to the ''frozen'' field profiles, as in Refs. 19 and 20.

## III. MODEL DESCRIPTION

### A. Geometry description and main formulas

Although in this paper we will deal with only uniform applied fields, here we introduce formulas for the general case of a nonuniform applied field, in order to use them in the levitation calculations. We consider a cylindrically symmetric external field $\mathbf{H}^a(\rho,z)$ applied over a cylindrical zero-field cooled superconductor of radius $R$ and length $L$ with the same axis of symmetry. We use common cylindrical coordinates $(\rho,\phi,z)$. We assume that the SC does not influence the sources of the external applied field.

The applied field can have neither an azimuthal component nor angular dependence. Its general expression is therefore

$$\mathbf{H}^a(\rho,z)=H_\rho^a(\rho,z)\hat{\rho}+H_z^a(\rho,z)\hat{z}. \tag{1}$$

Due to the cylindrical symmetry, any induced current will flow in the azimuthal direction $\mathbf{J}=J_\phi(\rho,z)\hat{\boldsymbol{\phi}}$. We model the superconductor as a set of $n\times m$ coaxial rings of rectangular section (see Fig. 1). Typical values used in this work are $n\times m=60\times 60$. We define $\Delta R=R/n$ and $\Delta L=L/m$. Each rectangular section has, thus, a surface $(\Delta R)(\Delta L)$. We consider that linear currents may flow through the center of that section with a value $I=J_c(\Delta R)(\Delta L)$. Due to the rotational symmetry of the problem, it is sufficient to find a solution at any of the (semi)planes of constant angle.

We assume the SC to be in the critical state. The applied fields $H_a$ will always be such that $H_{c1}\ll H_a\ll H_{c2}$. In general, we will consider a dependence of the critical current upon internal magnetic field, so $J_\phi=J_c(|\mathbf{H}_i|)$.

We now introduce some of the quantities involved in the model. In cylindrical geometry, only the vertical component of the magnetic field contributes to the total magnetic flux $\Phi_{ij}$ that threads the area closed by a current ring indexed as $ij$. There will be two contributions to the total flux: the internal flux $\Phi_{ij}^{int}$, created by the currents present in the super-

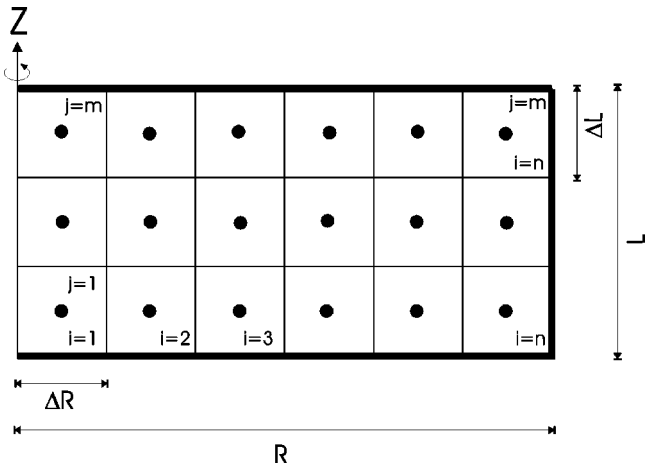


FIG. 1. Sketch of the division used in the simulation of a cylindrical superconductor. A semiplane of constant angle $\phi$ is shown. The points represent the linear circuits where current can flow.

conductor (including the current in the ring itself); and the external flux $\Phi_{ij}^{ext}$, due to the externally applied field. These magnitudes are calculated as

$$\Phi_{ij}^{int}=\sum_{kl} M_{kl,ij}I_{kl}, \tag{2}$$

$$\phi_{ij}^{ext}=2\pi\mu_0(\Delta R)\sum_{k\leqslant j} \rho_{ik}H_{z,ik}^{a}, \tag{3}$$

where $H_{z,ik}^{a}$ is the vertical component of the external applied field evaluated at the points where the current $ik$ flows, $\rho_{ik}$ is the radius of the circuit $ik$, $\rho_{ik}=(i-1/2)(\Delta R)$, and the coefficients $M_{kl,ij}$ are the mutual inductances between the circuits located at the circuits $kl$ and $ij$, which are calculated by the known formulas for linear circular circuits.[21]

The self-inductances are included in the summation of Eq. (2). It is known that the self-inductance of a strictly linear current diverges. This problem was solved in the literature in different ways (see Ref. 7, for example). In our work, we have calculated the self-inductances as the mutual inductances between two close linear circuits. We have considered two circuits of radius $\rho$ and $\rho+\epsilon$, calculated the mutual inductance between them, and found the value $\epsilon$ that fits this value with the one found by the expression for a linear circuit of section $\Delta R$.[22] We have found that the optimum choice for $\epsilon$ is $\epsilon\sim 0.78\Delta R$. As expected, as the mesh gets finer, the $\epsilon$ dependence of the results decreases. Actually, for the mesh sizes we have used, our results are, within numerical precision, independent of $\epsilon$.

The total density of magnetic flux, after a current profile is obtained, can be calculated either from the Biot-Savart formula or from the flux values. The axial component at a point indexed by $ij$ can be obtained from the flux as

$$B_{z,ij}=\frac{\Phi_{ij}-\Phi_{i-1j}}{\pi(\rho_{ij}^2-\rho_{i-1j}^2)}, \tag{4}$$

defining $\rho_{0j}=0$ and, thus, $\Phi_{i0}=0$. The radial component of the field can be calculated from the values of the axial component by imposing the condition that the divergence of **B** is equal to zero, so that

$$B_{r,ij}=\left[\frac{1}{(\Delta R)}+\frac{1}{\rho_{ij}}\right]^{-1}\left(\frac{B_{r,i-1j}}{(\Delta R)}+\frac{B_{z,ij}}{(\Delta L)}-\frac{B_{z,ij+1}}{(\Delta L)}\right), \tag{5}$$

with $B_{r,0j}=0$.

Since only azimuthal currents will be present in the superconductor, the magnetic moment created by them will have only axial component. We define the magnetization as the magnetic moment divided by the superconductor volume as

$$M_z=\frac{m_z}{\pi R^2 L}=\frac{1}{R^2 L}\sum_{ij}^{nm} I_{ij}\rho_{ij}^2. \tag{6}$$

The applied field enters into our calculations as shown in Eq. (3), which makes our approach free from the problems associated with implementing boundary conditions in points far from the superconductor or through a surface layer.[7] We would like to remark that an important advantage of the model is that it can be applied to nonuniform external fields, as studied in the second paper of this series.

### B. Uniform magnetic-field case

In the rest of this paper we will consider a uniform applied field of the form

$$\mathbf{H}^a=H_a\hat{\mathbf{z}}. \tag{7}$$

In this case, we will obtain symmetrical current and field profiles not only in the azimuthal direction but also with respect to the central layer of the superconductor.

As stated above, in the present procedure the external field only appears in Eq. (3), which in the constant applied field case is simplified as

$$\Phi_{ij}^{ext}=\mu_0\pi\rho_{ij}^2 H_a. \tag{8}$$

### C. Energy-minimization procedure

We now describe the method for obtaining the current and field profiles. We first focus on the Bean case (no field dependence for the critical current), leaving the introduction of a field dependence for Sec. III D.

We first consider the initial curve. Let us assume a given current distribution corresponding to an applied field $H_a$ (if we are calculating the first point after the initial state, then the initial current distribution is zero everywhere). Setting a current $I$ at a circuit indexed as $(i,j)$ requires an energy

$$E_{ij}=I\Phi_{ij}^{int}=I\sum_{kl} M_{kl,ij}I_{kl}, \tag{9}$$

while it contributes to reduce the energy (current has opposite sign to $H_a$) by a factor $I\Phi_{ij}^{ext}$. We find in this way the circuit that yields the largest decrease of energy, and set a

current $I$ there. Following Bean's critical state model, we put a current with value $I=J_c\Delta R\Delta L$.

This process is repeated until it becomes impossible to decrease the magnetic energy by setting a new current anywhere. Then, from the existing current profiles, we calculate **B** profiles from Eqs. (4) and (5) and the magnetization from Eq. (6). When $H_a$ is further increased, the same procedure starts again from the previous current values.

When the applied field has reached a maximum value $H_{\max}$ and is lowered, as we explained in Sec. II, we apply the same minimization procedure, taking into account only the currents induced during this reversal stage, that is, those induced due to the variation of the field from $H_{\max}$ to some $H_a<H_{\max}$, and we superpose these currents to the frozen ones in the interior. This procedure, typical of critical-state models, has been used in the literature in the two limit cases for which analytical expressions for the magnetization of superconducting cylinders can be found, that is, for infinite cylinders[16] and very thin disks.[17] This process yields a magnetization for the reverse curve $M_{\rm rev}(H_a,H_{\max})$ that is related to the initial magnetization curve $M(H)$ by[23]

$$M_{\rm rev}(H_a,H_{\max})=M(H_{\max})-2M\left(\frac{H_{\max}-H_a}{2}\right). \quad (10)$$

### D. $J_c(H_i)$ dependence

The previous procedure should be modified when we want to introduce some dependence of the critical current upon the internal magnetic field since, when $H_a$ changes, the internal field will also be modified, and therefore so will the value of the already induced currents. The $J_c(H_i)$ dependence could be introduced by means of an iterative algorithm. However, in our modelization we can increase the external applied field in amounts small enough as to consider that the new induced currents do not modify much the already induced ones during this step of variation of field. The procedure can be then regarded as just the first step of an iterative method. However, we have checked that this ''first iteration'' method is satisfactory by confirming that further iterations do not significantly modify the results provided that the applied field is increased in small steps.

The procedure consists in the following. After increasing the applied field, the new currents are set accomplishing the chosen material law $J_c(H_i)$. When no new current minimizes the energy further, we calculate the magnetic field inside the superconductor and change the value (not the distribution) of the already induced currents according to the material law. After this, the applied field can again be increased and the process restarted.

## IV. RESULTS FOR THE CONSTANT $J_c$ CASE

### A. Magnetization and current profiles: Sample size dependence

We first discuss the case of constant $J_c$ for simplicity. In Fig. 2 we show the calculated magnetization curves for superconducting cylinders with different length-to-radius $L/R$ values and the same critical current $J_c$. The applied field is normalized to the value $H_p=J_cR$, which corresponds to the penetration field for the infinite case, whereas the magnetization is normalized to $J_cR/3$, which corresponds to the saturation magnetization for all cases. This normalization makes the results independent of the particular values of $J_c$ and $R$.

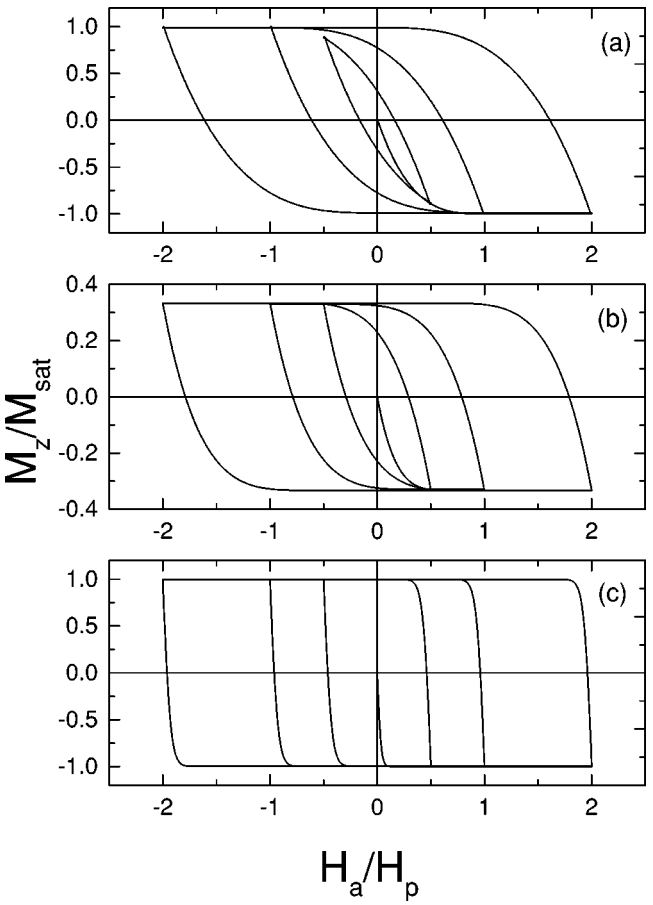


FIG. 2. Magnetization loops for constant critical current as a function of the applied field. (a) $L/R=10$. (b) $L/R=1$. (c) $L/R=0.1$.

The effect of the sample size is clearly displayed in the figure. For smaller $L/R$ ratios the loops present the main difference: the initial slopes in both the virgin and reverse curves become larger (in absolute value) with decreasing $L/R$. In relation to this, the saturation value (achieved when the superconductor becomes fully penetrated) is reached at lower applied fields for shorter samples. In all cases, when the SC is fully penetrated, the value of the magnetization is the same, since the saturation magnetization (the magnetic moment per volume) is independent of the $L/R$ value in the Bean approximation of a constant $J_c$.

In Fig. 3 we plot the calculated current penetration profiles for the three samples of Fig. 2 and for different applied fields, all in the initial curve. It can be seen that currents penetrate from the lateral surface to the interior and that the penetration close to both the bottom and end of the SC is deeper than in the central layer. This behavior is accentuated when $L/R$ decreases.

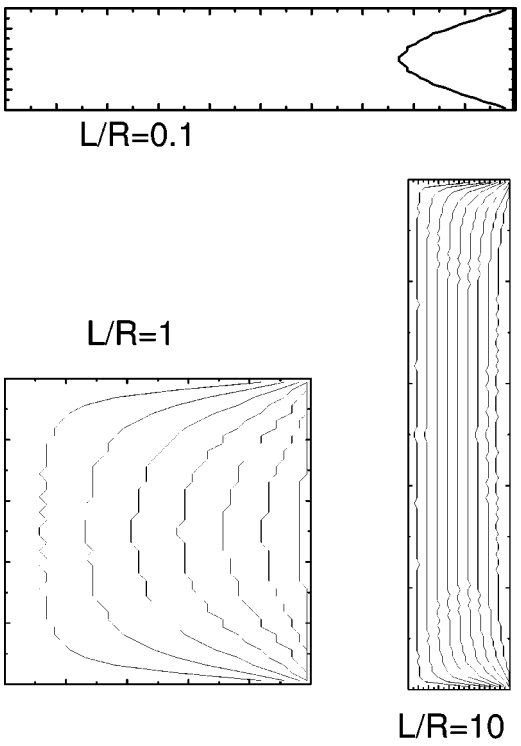


FIG. 3. Current profiles for three different cylinders. In each case the axis of the cylinder is at the right of each figure. For the cases $L/R=10$ and 0.1, the small dimension has been doubled for clarity.

### B. Current and field penetration in infinite and finite cylinders: Effect of demagnetizing fields

The features mentioned above result from the effects of the demagnetizing fields, and can be analyzed using the framework provided by our model. We shall first recall how the current and field behave throughout a hysteresis loop in the conventional critical state model, i.e., for an infinite cylinder in longitudinal applied field, and then see how the same process is understood in finite cylinders and why the discussed facts occur.

In a zero-field-cooled infinitely long superconducting cylinder, when a field $H_a$ is applied along the cylinder axis, currents are induced along the (infinitely long) lateral surface of the cylinder, creating a constant vertical field opposed to the applied one in the interior and a null field outside. Thus the interior region is shielded from the applied field, and in the exterior of the superconductor the total field is equal to the applied one. With a further increase of $H_a$, the current penetrates deeper into the cylinder, so that the shielded region shrinks. In this initial state of penetration the magnetization curve $M(H_a)$ is an increasing function (in absolute value) of $H_a$. At a field $H_p=J_cR$ the cylinder becomes fully penetrated by supercurrents.[4] As a consequence, since $J_c$ has a constant value, the sample magnetization (given by the magnetic moment created by supercurrents) cannot increase, and saturates. The reverse magnetization curve, obtained when reversing the sense of sweeping the applied field after reaching a maximum field $H_{\max}$, is understood in similar terms because, following the critical-state model, the reversal currents induced during this stage again shield the interior of the sample.[4,24,16] Thus the current and field distributions inside this shielded region remain frozen.

In a finite sample, as soon as the applied field $H_a$ is increased from zero, currents are induced in some of the superconductor regions in response to the field change. In this case, the depth of current penetration is not vertically the same, because a straight finite vertical penetration cannot shield a constant applied field in the internal region of a finite sample, assuming a constant current density. As seen in Fig. 3, near the ends of the superconductor, currents penetrate deeper into the superconductor. The current profiles in the finite case can be explained as follows. Since the superconductor tends to shield an internal region from a uniform applied field, the distribution of current should create a constant field inside the internal region. As stated, this cannot be achieved by a vertically constant profile. The currents appearing in the region close to the cylinder ends have to substitute for the effect of an infinitely long set of currents that is not present in a finite sample. This current distribution creates a field that modifies the external field everywhere (not only in the interior region, as in the infinite case). Therefore, outside the superconductor, the magnetic field is no longer $H_a$ except in points far from the superconductor.

In particular, the effect of the field produced by the first penetrated currents (in the corners) over the other loops is to increase the field in some regions, so that the real field in the lateral surface of the cylinder is larger than the applied field. As a result, the magnetization produced by such currents apparently corresponds to larger values of the applied field $H_a$. Thus the effect of this is to increase the slope of the initial $M(H_a)$ curve. The initial slope of the reverse curve is explained in the same way. Moreover, the thinner the sample, the larger the contribution from the end regions, and thus the larger the slope.

### C. Full penetration field

The process of penetration depends strongly on the sample size, as indicated above. In particular, the applied field at which the cylinder is totally penetrated, $H_{\rm pen}$, depends on $L/R$. Once the full penetration is reached, as long as the applied field is not decreased, the magnetization has a saturation value $M_{\rm sat}=J_cR/3$, independent of $L/R$.

By calculating the field caused by a full penetration of currents in finite cylinders, Forkl[25] obtained a formula for the penetration field $H_{\rm pen}$, which normalized to the penetration field of an infinite sample $J_cR$ as a function of the ratio $L/R$ is

$$\frac{H_{\rm pen}}{J_cR}=\frac{L}{2R}\ln\left[\frac{2R}{L}+\left(1+\frac{4R^2}{L^2}\right)^{1/2}\right]. \tag{11}$$

Our results for $H_{\rm pen}$ [which can be obtained either by finding the field at which the last possible current is set, or directly from the $M(H_a)$ data as the field at which the initial and the reverse curves merge] agree with the formula given by Forkl within our numerical accuracy for all values of $L/R$. In Sec. V we will study how $H_{\rm pen}$ changes when some dependence of $J_c$ upon $B$ is considered.

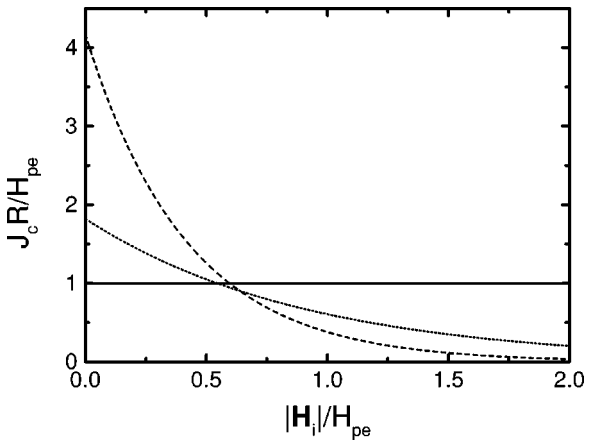


FIG. 4. Dependences of the critical current density $J_c$ as a funtion of the modulus of the internal field $|H_i|$ used in this series of papers. $J_c$ is normalized to the penetration field of an infinite cylinder $H_{pe}$ divided by cylinder radius $R$; $|H_i|$ is normalized to $H_{pe}$. Note that with the normalization shown, the function depends only on $p$. Solid, dotted, and dashed lines correspond to $p=0$, 2, and 10, respectively.

## V. RESULTS FOR THE $J_c(H_i)$ CASE

### A. Exponential dependence

As mentioned in the introduction, the critical state in most type-II superconductors is best described with a $J_c$ which depends on the local field $H_i=B/\mu_0$ at the current position. In this section we study the influence of demagnetizing fields in the realistic case of a material with a given $J_c(H_i)$ dependence. In this paper, the dependence will be of exponential type,[26,16]

$$J_c=k\exp(-|H_i|/H_{0e}), \tag{12}$$

where $k$ and $H_{0e}$ are positive constants, since this dependence is very adequate to describe magnetic properties of granular high-$T_c$ superconductors,[16,27,5] though our general framework allows the introduction of any arbitrary function $J_c(H_i)$. A useful parameter to describe the strength of the exponential decay of $J_c$ with $H_i$ is $p$, defined as[16]

$$p=kR/H_{0e}. \tag{13}$$

The limit $p\to 0$ corresponds to independent $J_c$ (Bean's model), and in general the larger $p$ is the stronger the dependence. Another useful parameter is $H_{pe}$, defined as

$$H_{pe}=H_{0e}\ln(1+p), \tag{14}$$

which corresponds to the field of total penetration in an infinite sample.

If the applied fields involved in the problem are normalized with $H_{pe}$ and the length dimensions with the radius $R$, then the results only depend on the $L/R$ ratio and the value of $p$. In Fig. 4 we plot the different shapes of $J_c(H_i)$ dependencies we will use in the following sections for studying how the variation on $p$ affects the shape of $J_c(H_i)$.

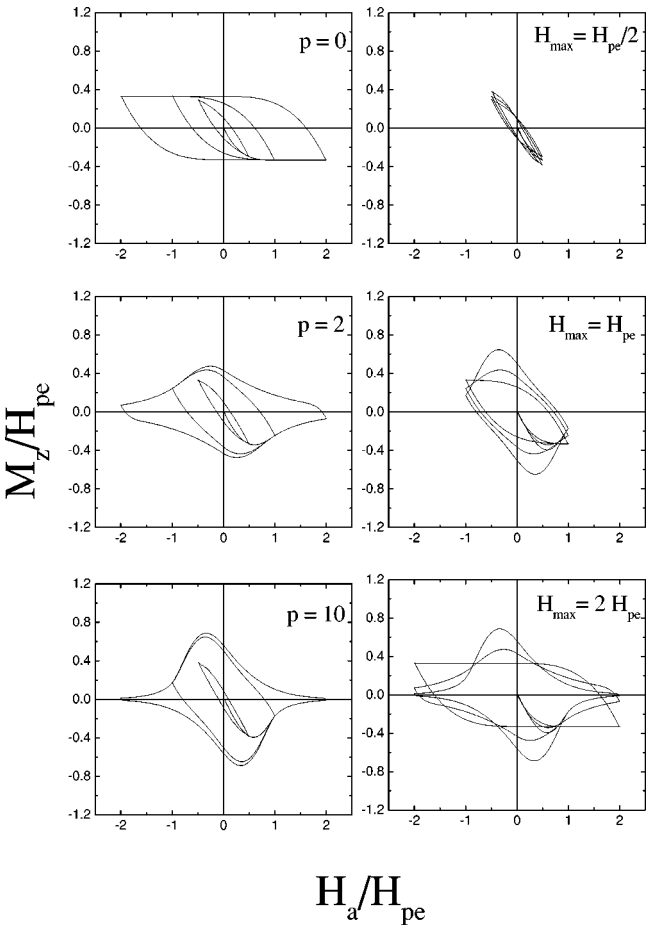


FIG. 5. Magnetization loops for a long sample $L/R=10$. In the left column each plot has a fixed value of $p$ (as shown) and different values of $H_{\max}/H_{pe}$ (0.5, 1, and 2). In the right column each plot has a fixed value of $H_{\max}/H_{pe}$ (as shown) and different values of $p$ ($p=0$, 2, and 10).

### B. Magnetization curves

#### *1. p dependence*

In Fig. 5 we show the calculated magnetization loops for the case $L/R=10$. Different values of $p$ have been used. For illustration we chose three values of $H_{\max}$: lower than, equal to, and higher than the penetration field $H_{pe}$ ($H_{\max}/H_{pe}=0.5$, 1, and 2, respectively). Our results are practically coincident with the analytical results for infinite samples, so we can regard the case $L/R=10$ as the infinitely long sample limit for discussions.

Figure 6 shows the dependence on $p$ of the magnetization loops calculated for a superconducting cylinder with $L/R=1$. Similar to the known results for infinite cylinders,[16,27] increasing the value of the parameter $p$ results in a decrease of the value of $M$ for high applied fields, and the appearance of a peak in the initial curve for fields lower than $H_{pe}$ and another one in the reverse curve at a negative field. The stronger the value of $p$ is, the sharper these peaks become. These features are general for any value of $L/R$, and their appearance can be explained as in the infinite case: when $p>0$, when the applied field is small, some currents penetrate into the superconductor with high value, and the magnetization increases (in absolute value). As the applied field in-

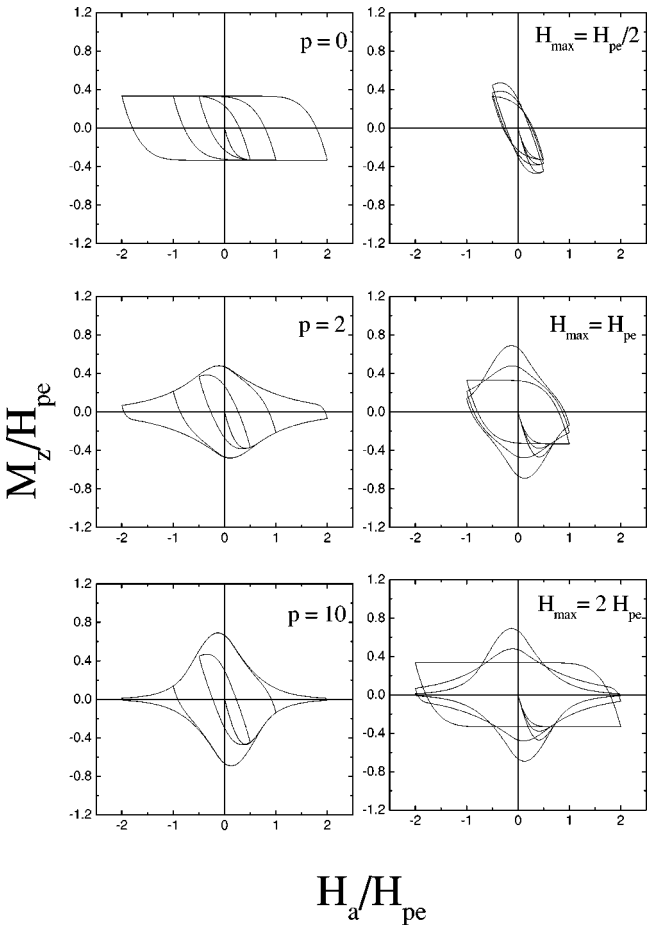


FIG. 6. Same as Fig. 5, for the case $L/R=1$.

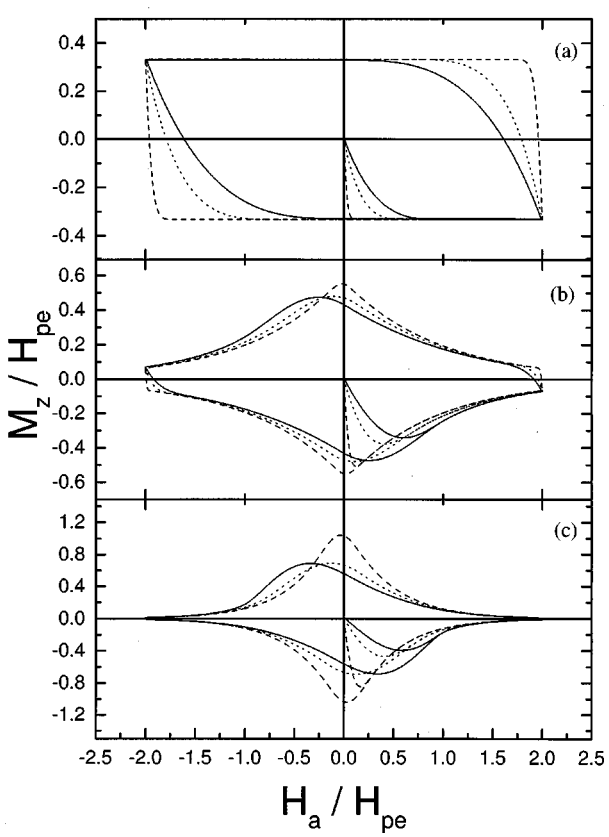


FIG. 7. Magnetization loops for different $p$: (a) $p=0$, (b) $p=2$, and (c) $p=10$. In each figure, solid line corresponds to $L/R=10$, the dotted line to $L/R=1$, and the dashed line to $L/R=0.1$.

creases further, so does the internal field; thus the value of the current decreases while it penetrates further. This produces two opposite effects: if the currents fill a larger volume the absolute value of the magnetization tends to increase, whereas if the current value decreases the value tends to decrease. A minimum in the initial magnetization appears when the relative importance of these two tendencies changes when increasing the applied field. Although the described behavior is general for all $L/R$ values, the demagnetizing fields arising from the finite size indeed have an actual influence in the results, as we discuss in Sec. V B 2.

#### *2. L/R dependence*

In Fig. 7 we show the calculated $M(H_a)$ curves displaying the dependence on $L/R$ for materials characterized by different values of $p$ [$p=0$ in Fig. 7(a), $p=2$ in Fig. 7(b), and $p=10$ in Fig. 7(c)]. For the sake of simplicity, we only show results for the case $H_{\max}/H_{pe}=2$.

Since in each figure $p$ has the same value, the observed differences between the different curves are associated only with shape effects and not with intrinsic properties. The general effect of the demagnetizing fields is that the thinner the sample, the larger the initial slope of the $M(H_a)$ in both the virgin and reverse curves (this is a general fact, independent of $p$), and thus the sharper the peak in the magnetization. Moreover, the peak shifts toward the $H_a=0$ axis. This effect was already found in theoretical calculations for thin strips[28] and disks[29] with a given $J_c(H_i)$ dependence, and also in experimental data for a Y-Ba-Cu-O thin film.[30] The physical reasons for this effect can be understood in the framework of our model, as explained in the following.

When $p=0$, induced supercurrents have a constant density and penetrate the superconductor, producing a certain magnetization, since the interior is shielded from the applied magnetic field. When $p>0$, as seen in Fig. 4, the supercurrent at low fields is larger in value than that corresponding to $p=0$; thus, to shield the same applied field, it penetrates a lesser distance inside the SC. The magnetization at lower fields is, thus, larger than in the $p=0$ case. The larger $p$ is the more accentuated this behavior becomes, and the larger the initial slope of the magnetization. When the applied field increases, and thus the internal field also tends to increase, the value of the current decreases and the magnetization attains a minimum value. When $L/R$ decreases, this minimum value is reached at lower external field values, because the demagnetization fields increase the internal field value (which is responsible for the dependence of $J_c$) above the applied field value. This explains the sharper peak at low $L/R$ values.

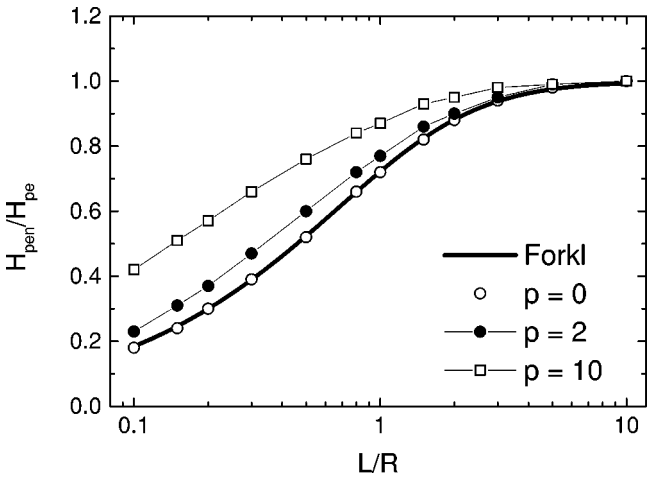


FIG. 8. Field of full penetration as a function of $L/R$. The solid line corresponds to Forkl's formula, and different labels to different values of $p$ as indicated in the figure.

### C. Penetration field for the $J_c(H_i)$ case

As explained in Sec. IV C, the field of full penetration depends on the $L/R$ value. It also depends on the $p$ value. In Fig. 8 we plot the calculated full penetration field normalized to the field of full penetration of an infinite sample $H_{pe}$ (for each $p$), as a function of $L/R$ and for different values of $p$. Forkl's formula corresponding to the $p=0$ case [Eq. (11)] is also plotted for comparison.

As seen in Fig. 8, our results for the case $p=0$ coincide with the analytical expression of Eq. (11). When $p>0$ the field of full penetration decreases when the sample becomes shorter. This fact is due to the demagnetization effects as in the case $p=0$. For a given $L/R$, it is seen that $H_{\rm pen}/H_{pe}$ increases with increasing $p$ (being, obviously, 1 when $L/R \gg 1$ for all $p$'s). For large $p$ at low fields, currents have high value and penetrate less, so the field of penetration is expected to be larger. The thinner the sample, the more accentuated this behavior becomes, since full penetration is attained at lower fields.

### D. Extraction of the $J_c(H_i)$ function from the experimental magnetization curve

The function $J_c(H_i)$ is often extracted from measurements of the magnetization loops of superconducting cylinders by applying the formula $J_c(H)=3\Delta M(H)/2R$, where $\Delta M(H)$ is the width of the loop at the applied field $H$. This formula is known to be valid when the internal field is not very different from the applied one, and when the superconductor is fully penetrated.[24,31] Moreover, its use has been justified until now only for infinite samples.

When demagnetization effects are present, extracting the intrinsic dependence $J_c(H_i)$ is complicated since the internal field is in general not uniform. Our results show that in general a good agreement between the actual and the magnetically extracted $J_c(H_i)$ function is found for fields larger than the penetration field, as discussed in Ref. 32. Since the penetration field decreases drastically when decreasing the $L/R$ ratio, we find that samples with a large aspect ratio and a transverse applied field will have a very small penetration field and are therefore ideal for experimentally extract the $J_c(H_i)$ function from magnetization measurements. This is especially true if the expected dependence is strong. A detailed treatment of this topic can be found in Ref. 33.

### E. Current profiles

In this section, we calculate the current profiles corresponding to some of the studied cases in order to see how the current distribution depends on $L/R$ and $p$. In Fig. 9 we show the $p$ dependence of the penetration profiles for the case $L/R=1$. As discussed above, we find that the effect of the finite size over the current profile is to increase the deep of penetration in the regions near the ends of the cylinder. It is also observed that when $p=0$ the current penetration depth in the central layer is a linear function of the applied field [as indicated by the constant separation between two consecutive lines; see Fig. 9(a)], as happens in the current-penetrated region in an infinite sample in Bean's critical state. When $p>0$ the behavior is different: at low fields the current profile penetrates less (for a given applied field) because the value of the current is higher (see Fig. 4), whereas, as the field is increased, the value of the current decreases and the current penetrates more deeply for a given field increment, as shown in Figs. 9(b) and Fig. 9(c). Obviously, the larger $p$ is the more accentuated this behavior becomes.

Current profiles for the reverse curve are displayed with thin lines in Fig. 9. In this reverse stage, the behavior is just the opposite of that for the initial curve: since at the early stage the fields are large, the current is low and has to penetrate deeper in order to shield a given field variation. As the applied field decreases the current value increases, and the distance between two consecutive field profiles is reduced. When the field decreases to negative values the current value increases and the profiles separate again. This behavior is, of course, more evident for large $p$, as can be seen in Fig. 9(c). For the constant current case ($p=0$), the depth of current penetration in the central layer resulting from a given field step is always the same, independently of the particular applied field value.

## VI. DISCUSSION

### A. Comparison with experiments, model checks and limits

The procedure we have described is based on the minimization of the magnetic energy of a system of currents which represents the superconductor. There were, recently several other alternative methods presented in the literature to solve the critical-state problem in cylinders. The magnetization and the current profiles we have found using our method have been checked with those from other models, whenever comparable results exist, as we briefly summarize in this section.

The method calculates the field of full penetration. For $p=0$, our results coincide with those by Forkl, as discussed in Sec. III C.

We obtain the same values for the initial slope of the $M(H_a)$ curves as those calculated by Brandt[7] and Chen

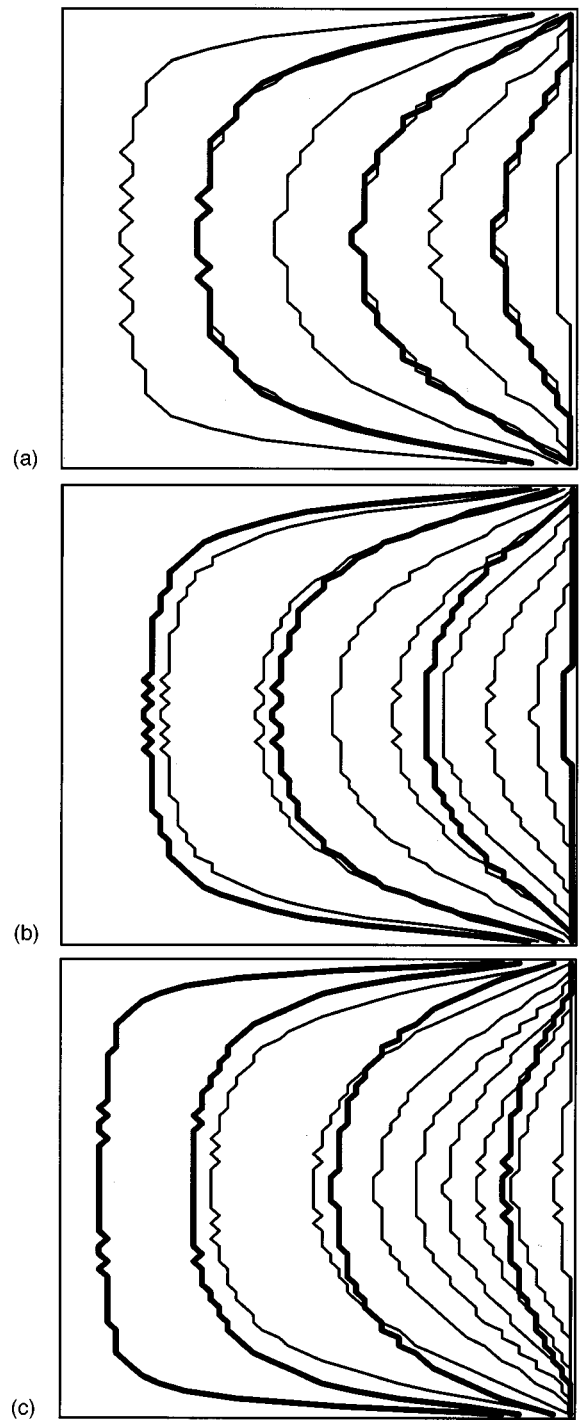


FIG. 9. Calculated current profiles for the case $L/R=1$, for different values of $p$: $p=0$ (top), 2 (middle), and 10 (bottom). Thick and thin lines represent the profiles in the initial and reverse magnetization curves, respectively. The axis of the cylinder is shown in the right. The applied field is increased (and decreased) from 0 to $H_{\max}=2H_{pe}$ in steps of $0.1H_{pe}$.

*et al.*[34] for a wide range of $L/R$ values, with less than a 1% deviation (for the comparison with the data of Chen *et al.* one should use their results for $-1$ susceptibility). The agreement has been also shown to exist when comparing our data with experimental results of niobium cylinders (a detailed discussion on this can be found in Ref. 35).

The case of long samples gives correct results when comparing with results for Bean's model[4] for the case of constant critical current and with those of Ref. 16 for the exponential dependence. In the opposite limit of very thin disks, our calculated current profiles, averaged over the superconductor thickness, are coincident within numerical precision with the analytical results of Ref. 17 for the studied case of $p=0$, whereas, for the $J_c(H_i)$ case, our magnetization curves agree, within numerical precision, with the ones numerically calculated by Shantsev *et al.*[29,36]

For finite cylinders, some of the profiles and magnetization curves for the case $p=0$ were also calculated by Brandt[7] using a different numerical approach. Within numerical accuracy, our results coincide with his.

### B. Model extensions

An important advantage of our model is that it is equally applicable to any form of the applied magnetic field, as long as it keeps the cylindrical symmetry. In the following paper (part II) we present an application of our method to the case of an inhomogeneous applied magnetic field, that of a permanent magnet, which allows us to calculate the current and field profiles and levitation force in the superconductor.

However, our procedure is not applicable for an arbitrary applied field, because the trajectories followed by supercurrents are in general not known *a priori*. Nevertheless, if by some means a way of obtaining such trajectories is developed, our approach could be used to solve the general (three-dimensional) problem of current penetration in samples of arbitrary shape in an arbitrary applied field. The main equations would remain the same, and only the mutual inductance coefficients (which are always expressable in terms of easy numerically computed integrals) corresponding to the particular current trajectories would have to be input in the equations.

## VII. CONCLUSIONS

We have presented a model for understanding the process of current and field penetration in finite type-II superconducting cylinders. One of its advantages is that in order to understand the physical effects of demagnetizing fields one does not need to rely on complicated distributions of surface poles, but instead the complete magnetic field distribution can be obtained as the linear superposition of fields created by simple current loops. Our process is noniterative for constant $J_c$, and with a simple one-step iteration for $J_c(H_i)$.

The effects of demagnetizing fields in the magnetic response of the superconductor have been systematically analyzed. In particular, in a first step we have discussed the dependence of the magnetization loops upon the cylinder aspect ratio for a constant critical-current density, whereas in a second step we have added the effect of the dependence of the critical-current density upon the internal field.

Our model represents an alternative to other recent approaches for calculating the magnetic response of finite superconductors. Our approach is especially adequate for studying the case of a nonuniform applied field as required in levitation experiments, as we show in the following paper.

**ACKNOWLEDGMENTS**

We acknowledge DGES Project No. PB96-1143, Ministerio de Ciencia y Tecnología Project No. BFM2000-0001, and CIRIT Project No. 1999SGR00340 for financial support.

[1] E.H. Brandt, Science **243**, 349 (1989).
[2] J.R. Hull, Supercond. Sci. Technol. **13**, R1 (2000).
[3] F.C. Moon, *Superconducting Levitation* (Wiley, New York, 1994).
[4] C.P. Bean, Rev. Mod. Phys. **36**, 31 (1964); Phys. Rev. Lett. **8**, 250 (1962).
[5] D.-X. Chen and A. Sanchez, J. Appl. Phys. **70**, 5463 (1991).
[6] A. Sanchez, D.-X. Chen, J.S. Muñoz, and Y.-Z. Li, Physica C **175**, 33 (1991).
[7] E.H. Brandt, Phys. Rev. B **58**, 6506 (1998).
[8] T.B. Doyle, R. Labusch, and R.A. Doyle, Physica C **290**, 148 (1997).
[9] T. Torng and Q.Y. Chen, J. Appl. Phys. **73**, 1198 (1992).
[10] P. Shönhuber and F.C. Moon, Appl. Supercond. **2**, 523 (1994).
[11] W.C. Chan, D.S. Jwo, Y.F. Lin, and Y. Huang, Physica C **230**, 349 (1994).
[12] A. Sanchez and C. Navau, Physica C **268**, 46 (1996).
[13] C. Navau and A. Sanchez, Phys. Rev. B **58**, 963 (1998).
[14] A.B. Riise, T.H. Johansen, H. Bratsberg, M.R. Koblischka, and Y.Q. Shen, Phys. Rev. B **60**, 9855 (1999).
[15] A. Sanchez and C. Navau, Physica C **275**, 322 (1996).
[16] D.-X. Chen, A. Sanchez, and J.S. Muñoz, J. Appl. Phys. **67**, 3430 (1990).
[17] J.R. Clem and A. Sanchez, Phys. Rev. B **50**, 9355 (1994).
[18] A. Badia, C. Lopez, and J.L. Giordano, Phys. Rev. B **58**, 9440 (1998).
[19] E.H. Brandt and M. Indenbom, Phys. Rev. B **48**, 12 893 (1993).
[20] E. Zeldov, J.R. Clem, M. McElfresh, and M. Darwin, Phys. Rev. B **49**, 9802 (1994).
[21] J. D. Jackson, *Classical Electrodynamics* (Wiley, New York, 1975).
[22] L. D. Landau, E. M. Lifshitz, and L. P. Pitaevskii, *Electrodynamics of Continuous Media*, 2nd ed. (Pergamon Press, New York, 1984).
[23] E.H. Brandt, Phys. Rev. B **55**, 14 513 (1997).
[24] D.-X. Chen and R.B. Goldfarb, J. Appl. Phys. **66**, 2489 (1989).
[25] A. Forkl, Phys. Scr. **T49**, 148 (1993).
[26] W.A. Fietz and W.W. Webb, Phys. Rev. **178**, 178 (1969).
[27] D.-X. Chen, A. Sanchez, J. Nogués, and J.S. Muñoz, Phys. Rev. B **41**, 9510 (1990).
[28] J. McDonald and J.R. Clem, Phys. Rev. B **53**, 8643 (1996).
[29] D.V. Shantsev, Y.M. Galperin, and T.H. Johansen, Phys. Rev. B **61**, 9699 (2000).
[30] D.V. Shantsev, M.R. Koblischka, Y.M. Galperin, T.H. Johansen, P. Nalevka, and M. Jirsa, Phys. Rev. Lett. **82**, 2947 (1999).
[31] T.H. Johansen and H. Bratsberg, J. Appl. Phys. **77**, 3945 (1995).
[32] M. Daumling and D.C. Larbalestier, Phys. Rev. B **40**, 9350 (1989).
[33] A. Sanchez and C. Navau, Supercond. Sci. Technol. **14**, 444 (2001).
[34] D.-X. Chen, J.A. Brug, and R.B. Goldfarb, IEEE Trans. Magn. **27**, 3601 (1991).
[35] F.M. Araujo-Moreira, C. Navau, and A. Sanchez, Phys. Rev. B **61**, 634 (2000).
[36] D.V. Shantsev, Y.M. Galperin, and T.H. Johansen, Phys. Rev. B **60**, 13112 (1999).